

# Spectroscopy and Amplitude Analysis at LHCb

MIKHAIL MIKHASENKO

on behalf of LHCb Collaboration

PWA/ATHOS 2019, Rio (Brazil)

September 2<sup>nd</sup>, 2019



# LHCb

auty

Ring Imaging CHerenkov

Kaon ID ~ 95%  
pi/K mis ID ~ 5%

Dipole Magnet

Hadronic CALorimeter

Muon Stations

Muon ID ~ 97%  
pi/mu mis ID ~ 1-3%

Vertex Locator

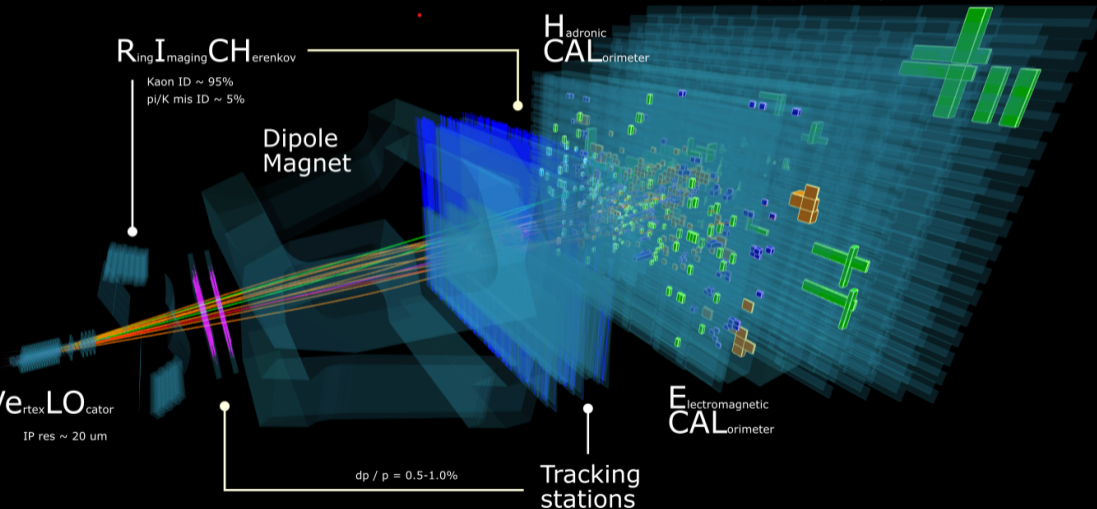
IP res ~ 20  $\mu\text{m}$

$dp/p = 0.5-1.0\%$

Tracking stations

Electromagnetic CALorimeter

pp collider (7+7 TeV)



# Spectroscopy and amplitude analysis

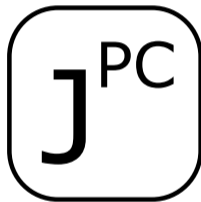
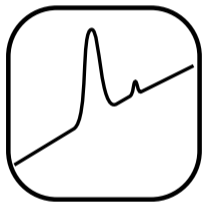
## Main motivation

Establishing pattern of QCD  
Search of exotic states

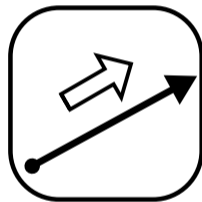
Polarization  
measurements



Studies of the CP violation  
in components



Determination of quantum  
numbers in decays



# Tools of LHCb experiment

## Techniques at every analysis

- Reaction specific kinematic fit (displaced vertices, invariant masses)
- BDTG by ROOT-TMVA trained from MC(signal) + side bands(bgd)

# Tools of LHCb experiment

## Techniques at every analysis

- Reaction specific kinematic fit (displaced vertices, invariant masses)
- BDTG by ROOT-TMVA trained from MC(signal) + side bands(bgd)
- Spectrum description:
  - ▶ Gauss $\oplus$ Crystal Ball, ARGUS $\otimes$ Gauss, exponent for bgd,
  - ▶ Feed-down – MC of missing particles.
  - ▶ single pole BW, relativistic BW, dedicated  $(\pi\pi/KK)_S$ ,  $(\pi K)_S$ ,  $(\pi D)_S$ .

# Tools of LHCb experiment

## Techniques at every analysis

- Reaction specific kinematic fit (displaced vertices, invariant masses)
- BDTG by ROOT-TMVA trained from MC(signal) + side bands(bgd)
- Spectrum description:
  - ▶ Gauss $\oplus$ Crystal Ball, ARGUS $\otimes$ Gauss, exponent for bgd,
  - ▶ Feed-down – MC of missing particles.
  - ▶ single pole BW, relativistic BW, dedicated  $(\pi\pi/KK)_S$ ,  $(\pi K)_S$ ,  $(\pi D)_S$ .
- **Amplitude analysis**

- ▶ Concept for the multibody decay – sum of truncated PW series:

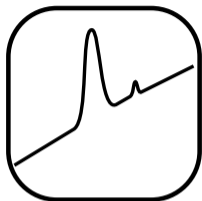
$$0 \rightarrow 123 : \quad M = M^{0 \rightarrow 1(23)} + M^{0 \rightarrow 2(31)} + M^{0 \rightarrow 3(12)},$$

- ▶ Formalisms: Helicity by Jacob-Wick, 3-tensors Zemach, covariant.

$$d_{\nu\lambda} \quad T_{ij\dots}(\vec{p}, \vec{q}) \quad O_{\mu\nu\dots}(P, Q)$$

- ▶ Common frameworks: Laura++, GooFit, TensorFlowAnalysis, ...

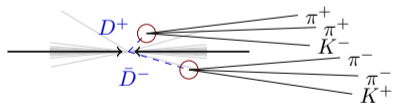
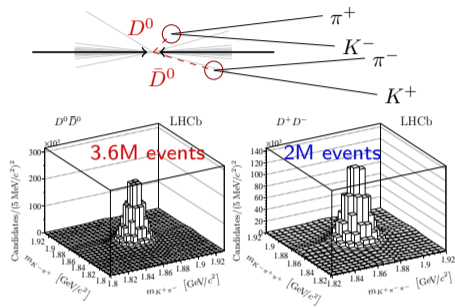
[arXiv:1711.09854], [GooFit-GitHub](#), [TFA-GitLab](#), ...



# New narrow charmonium state $X(3842)$

[JHEP 07 (2019) 035]

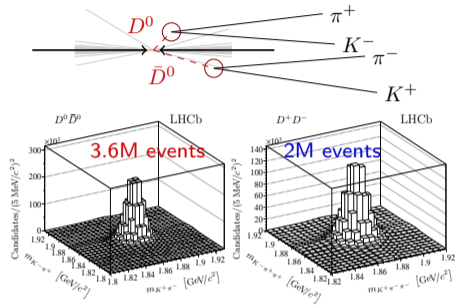
- kinematic fit, BDT, spectrum fit, feed-down



- displaced vertices
- 80 – 90 % purity

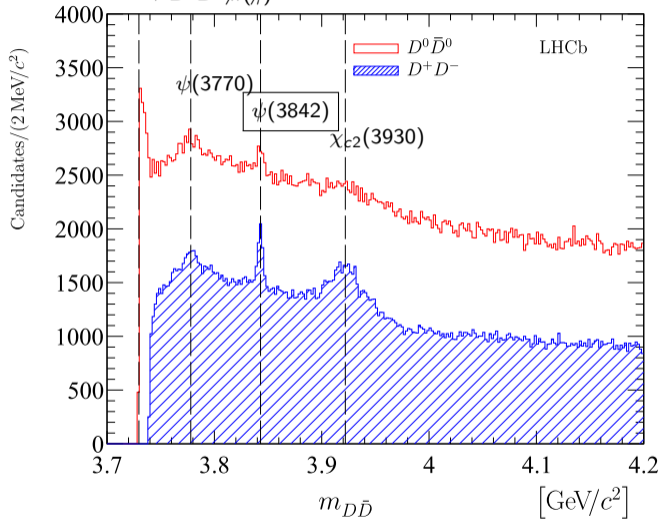


# Near threshold $D\bar{D}$ spectroscopy

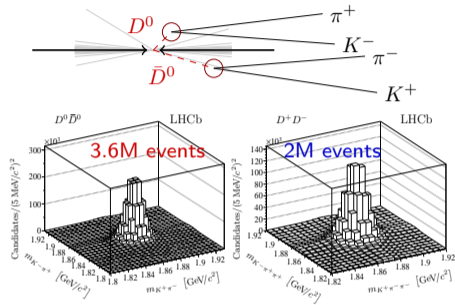


- displaced vertices
- 80 – 90 % purity

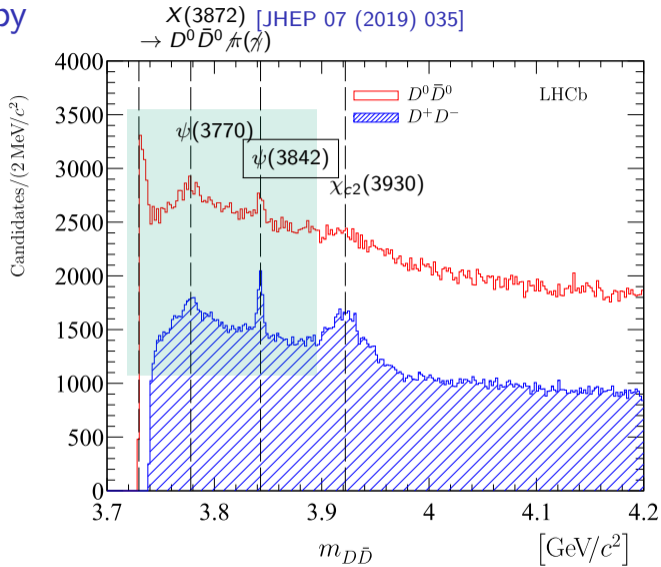
$X(3872)$  [JHEP 07 (2019) 035]  
 $\rightarrow D^0\bar{D}^0\pi(\pi')$



# Near threshold $D\bar{D}$ spectroscopy



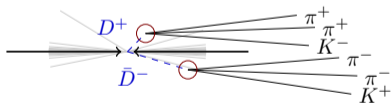
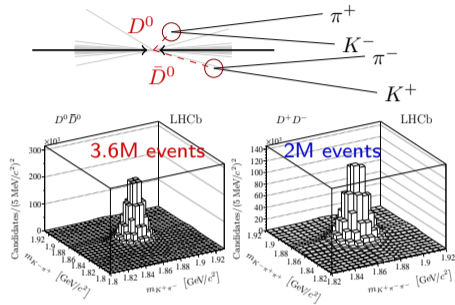
- displaced vertices
- 80 – 90 % purity



New state is consistent with  $1^3 D_3$  ( $\psi_3(1D)$ ),  $J^{PC} = 3^{--}$ .

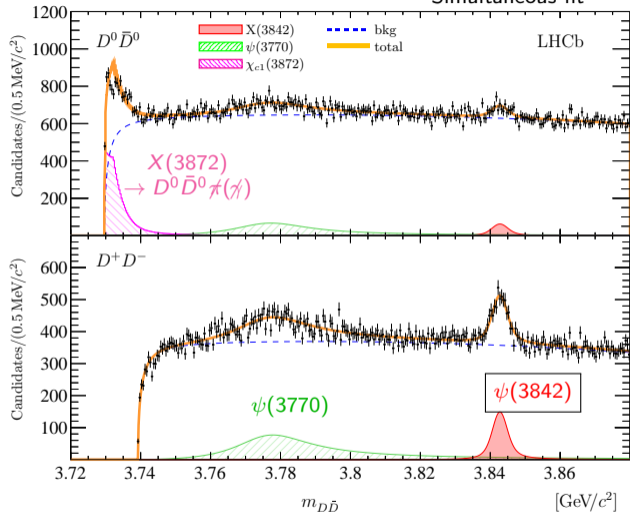
# Near threshold $D\bar{D}$ spectroscopy

[JHEP 07 (2019) 035]



- displaced vertices
- 80 – 90 % purity

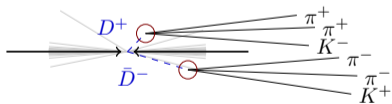
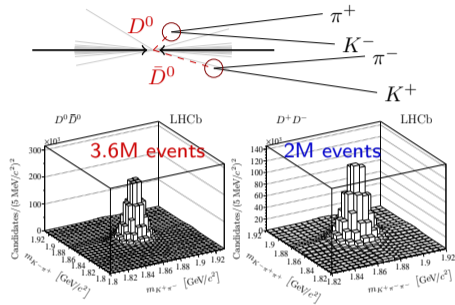
Simultaneous fit



New state is consistent with  $1^3 D_3$  ( $\psi_3(1D)$ ),  $J^{PC} = 3^{--}$ .

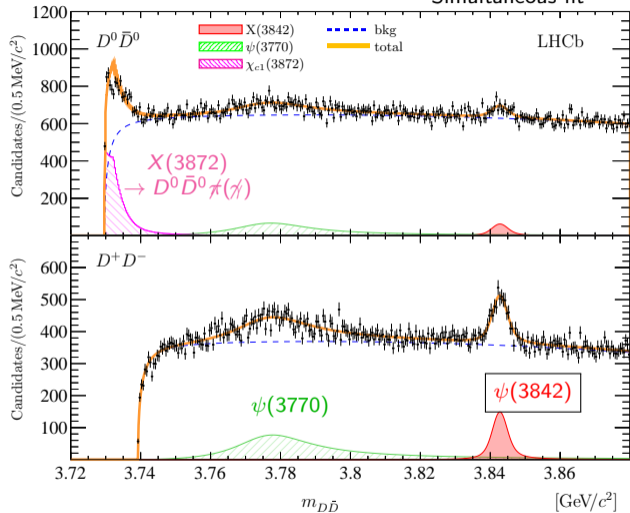
# Near threshold $D\bar{D}$ spectroscopy

[JHEP 07 (2019) 035]



- displaced vertices
- 80 – 90 % purity

Simultaneous fit



New state is consistent with  $1^3 D_3$  ( $\psi_3(1D)$ ),  $J^{PC} = 3^{--}$ .



# Origin of CP violation in $B^{\pm} \rightarrow h^{\pm} h^{+} h^{-}$

- kinematic constants, BDT, spectrum fit

# Direct CP violation in $B$ decays

[PRD 90, 112004 (2014)]

Appearance of CPV effects:

$$B \rightarrow f : A = \sum_i |A_i| e^{i(\delta_i + \phi_i)}$$

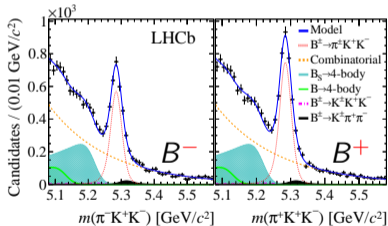
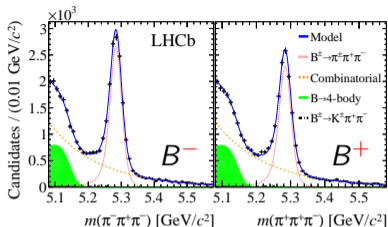
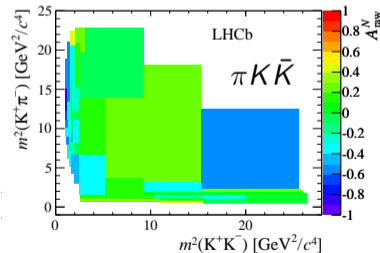
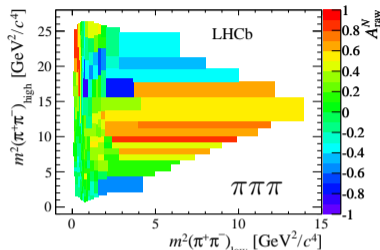
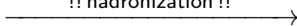
$$\bar{B} \rightarrow \bar{f} : \bar{A} = \sum_i |A_i| e^{i(\delta_i - \phi_i)},$$

- Strong phase ( $\delta$ ) does not change under CP,
- Weak phase ( $\phi$ ) flip the sign.

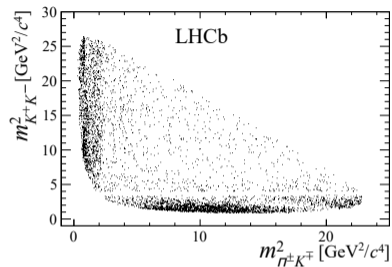
$$A_{CP} = \frac{|A|^2 - |\bar{A}|^2}{|A|^2 + |\bar{A}|^2}$$

$$\rightarrow \sum_i |A_i| |A_j| \sin(\delta_i - \delta_j) \sin(\phi_i - \phi_j)$$

!! hadronization !!



(see a talk of Patricia Magalhães on Thursday for details on  $B \rightarrow 3\pi$ ,  $D \rightarrow 3\pi$ ).

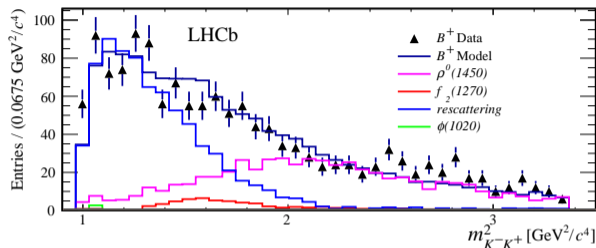
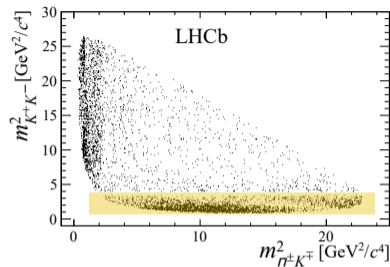


Fit-model components:

- $K^*(892)$ ,  $K^*(1430)$ ,  $f_2(1270)$ ,  $\rho(1450)$ ,
- phenom.  $(K\bar{K})_S$  and  $(K\pi)_S$ 
  - ▶  $(K\pi)_S$ : a left-hand pole  $(1 \text{ GeV}^2 + m_{K\pi}^2)^{-1}$
  - ▶  $(K\bar{K})_S$ : LH pole  $\times f_{\pi\pi \rightarrow K\bar{K}}^{(\text{Pelaez et al.})}$

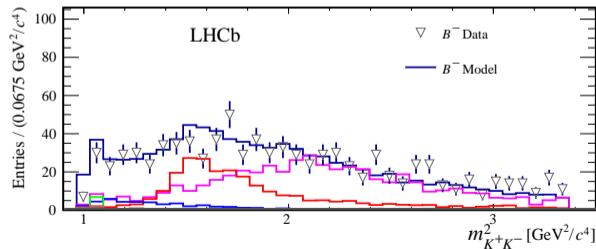
# Amplitude Analysis of $B^\pm \rightarrow \pi^\pm K^+ K^-$

[arXiv:1905.09244 (sent to PRL)]



Fit-model components:

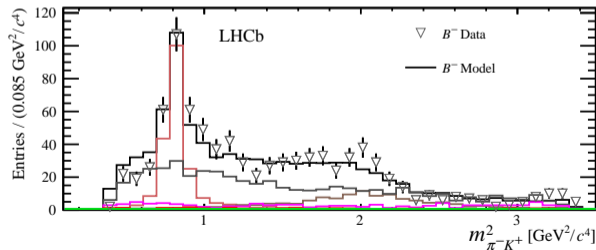
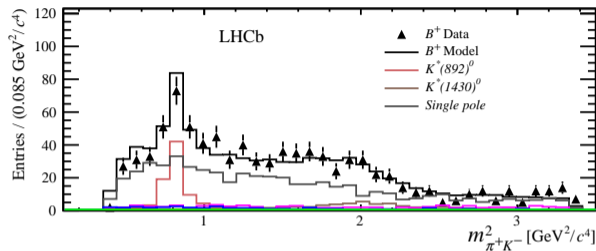
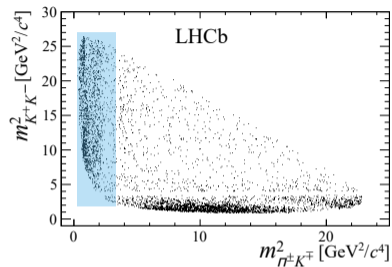
- $K^*(892)$ ,  $K^*(1430)$ ,  $f_2(1270)$ ,  $\rho(1450)$ ,
- phenom.  $(K\bar{K})_S$  and  $(K\pi)_S$ 
  - ▶  $(K\pi)_S$ : a left-hand pole  $(1 \text{ GeV}^2 + m_{K\pi}^2)^{-1}$
  - ▶  $(K\bar{K})_S$ : LH pole  $\times f_{\pi\pi \rightarrow K\bar{K}}^{(\text{Pelaez et al.})}$





# Amplitude Analysis of $B^\pm \rightarrow \pi^\pm K^+ K^-$

[arXiv:1905.09244 (sent to PRL)]

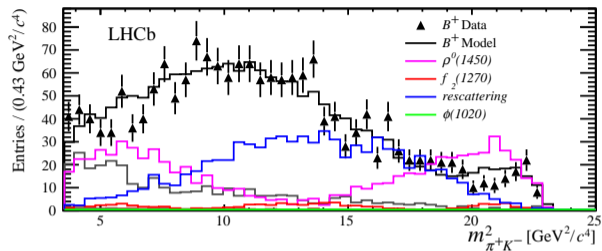
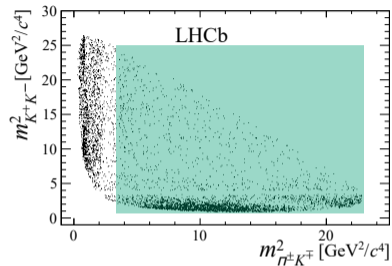


Fit-model components:

- $K^*(892)$ ,  $K^*(1430)$ ,  $f_2(1270)$ ,  $\rho(1450)$ ,
- phenom.  $(K\bar{K})_S$  and  $(K\pi)_S$ 
  - ▶  $(K\pi)_S$ : a left-hand pole  $(1 \text{ GeV}^2 + m_{K\pi}^2)^{-1}$
  - ▶  $(K\bar{K})_S$ : LH pole  $\times f_{\pi\pi \rightarrow K\bar{K}}^{(\text{Pelaez et al.})}$

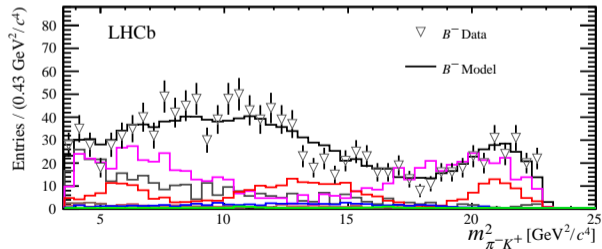
# Amplitude Analysis of $B^\pm \rightarrow \pi^\pm K^+ K^-$

[arXiv:1905.09244 (sent to PRL)]



Fit-model components:

- $K^*(892)$ ,  $K^*(1430)$ ,  $f_2(1270)$ ,  $\rho(1450)$ ,
- phenom.  $(K\bar{K})_S$  and  $(K\pi)_S$ 
  - ▶  $(K\pi)_S$ : a left-hand pole  $(1 \text{ GeV}^2 + m_{K\pi}^2)^{-1}$
  - ▶  $(K\bar{K})_S$ : LH pole  $\times f_{\pi\pi \rightarrow K\bar{K}}^{(\text{Pelaez et al.})}$

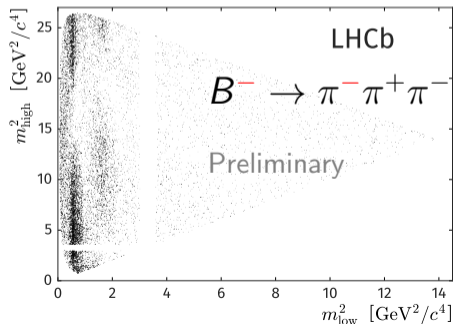
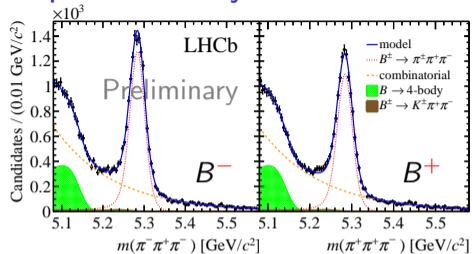


# Amplitude analysis of $B \rightarrow 3\pi$

[PAPER-2019-017 (LHCb), PAPER-2019-018 (LHCb)]

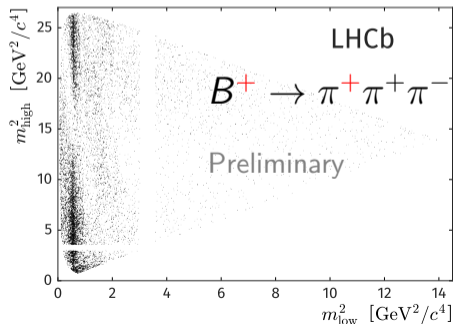
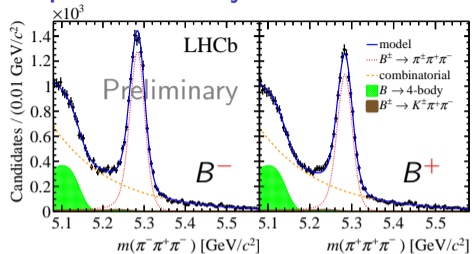
# Amplitude analysis of $B \rightarrow 3\pi$

[PAPER-2019-017 (LHCb), PAPER-2019-018 (LHCb)]



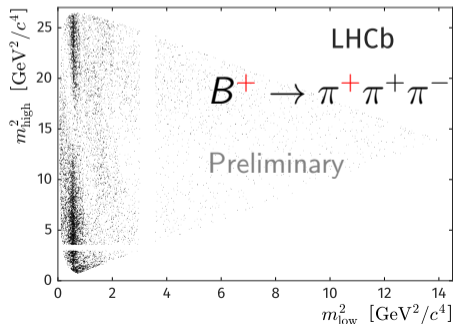
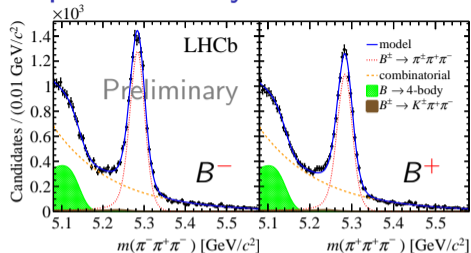
# Amplitude analysis of $B \rightarrow 3\pi$

[PAPER-2019-017 (LHCb), PAPER-2019-018 (LHCb)]



# Amplitude analysis of $B \rightarrow 3\pi$

[PAPER-2019-017 (LHCb), PAPER-2019-018 (LHCb)]

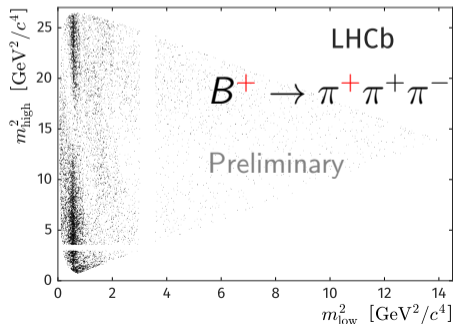
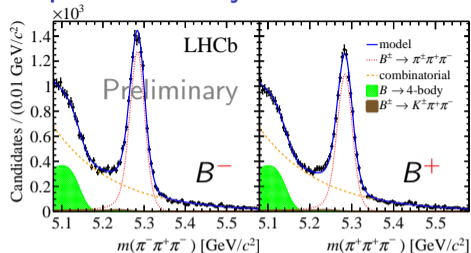


Amplitude analysis to investigate the origin:

- $\rho(770)$  with  $\omega$  interference
- $f_2(1260)$  and  $\rho_3(1690)$  by the RBW
- $(\pi\pi)_S$  coupled to  $K\bar{K}$ 
  - ① BW for  $\sigma + \text{LH pole} \times f_{\pi\pi \rightarrow K\bar{K}}^{(\text{Pelaez et al.})}$
  - ②  $P$ -vector with  $K$ -matrix by Anisovich-Sarantsev.
  - ③ binned freed lineshape (QMI)

# Amplitude analysis of $B \rightarrow 3\pi$

[PAPER-2019-017 (LHCb), PAPER-2019-018 (LHCb)]



Amplitude analysis to investigate the origin:

- $\rho(770)$  with  $\omega$  interference
- $f_2(1260)$  and  $\rho_3(1690)$  by the RBW
- $(\pi\pi)_S$  coupled to  $K\bar{K}$ 
  - ① BW for  $\sigma$  + LH pole  $\times f_{\pi\pi \rightarrow K\bar{K}}^{(\text{Pelaez et al.})}$
  - ②  $P$ -vector with  $K$ -matrix by Anisovich-Sarantsev.
  - ③ binned freed lineshape (QMI)

Several sources of the CP violation are observed:

- $(\pi\pi)_S$ -wave (in 2 slides)
- $\rho(770)/(\pi\pi)_S$  interference
- $f_2(1260)$

# $K$ -matrix parametrization

Anisovich-Sarantsev model fit to scattering data [EPJ A16 (2003)]

- Scattering — five-channel  $K$ -matrix ( $\pi\pi$ ,  $K\bar{K}$ ,  $4\pi$ ,  $\eta\eta$ ,  $\eta\eta'$ )
- $P$ -vector for the production amplitude  $F = P(1 - i\rho K)^{-1}$

$$K_{ij}(s) = \left( \sum_R \frac{g_j^{(R)} g_i^{(R)}}{m_R^2 - s} + \frac{b_{ij}^{\text{scatt}}}{s + s_0} \right) f_{A0}(s) \quad P_i(s) = \sum_R \frac{\beta^{(R)} g_i^{(R)}}{m_R^2 - s} + \frac{b_i^{\text{prod}}}{s + s_0}$$

- ▶  $g_i^R$ ,  $b_{ij}^{\text{scatt}}$  are constants fixed in the original work,
- ▶  $b_i^{\text{prod}}$ ,  $\beta^{(R)}$  are reaction-specific fit parameters;
- ▶  $f_{A0}(s)$  — Adler-zero term (rational).



# K-matrix parametrization

Anisovich-Sarantsev model fit to scattering data [EPJ A16 (2003)]

- Scattering — five-channel K-matrix ( $\pi\pi$ ,  $K\bar{K}$ ,  $4\pi$ ,  $\eta\eta$ ,  $\eta\eta'$ )
- P-vector for the production amplitude  $F = P(1 - i\rho K)^{-1}$

$$K_{ij}(s) = \left( \sum_R \frac{g_j^{(R)} g_i^{(R)}}{m_R^2 - s} + \frac{b_{ij}^{\text{scatt}}}{s + s_0} \right) f_{A0}(s) \quad P_i(s) = \sum_R \frac{\beta^{(R)} g_i^{(R)}}{m_R^2 - s} + \frac{b_i^{\text{prod}}}{s + s_0}$$

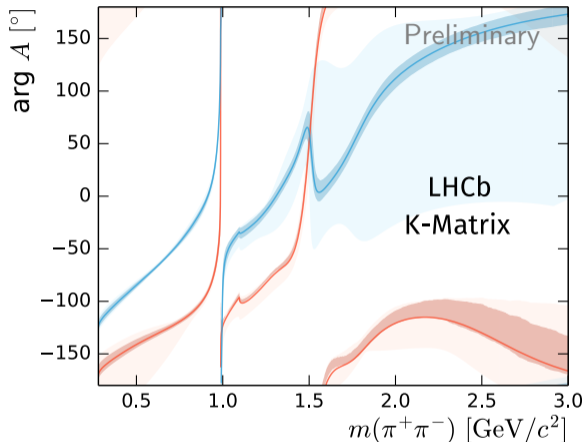
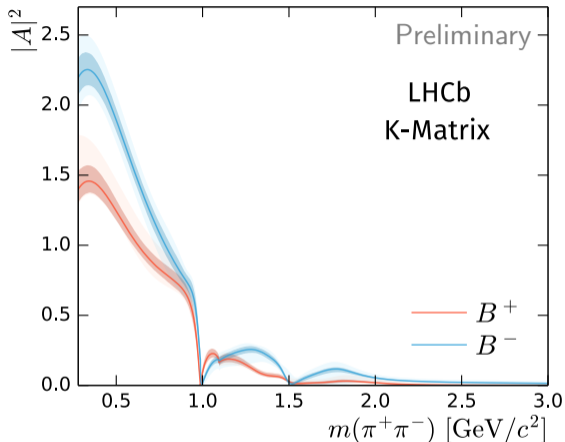
- ▶  $g_i^R$ ,  $b_{ij}^{\text{scatt}}$  are constants fixed in the original work,
- ▶  $b_i^{\text{prod}}$ ,  $\beta^{(R)}$  are reaction-specific fit parameters;
- ▶  $f_{A0}(s)$  — Adler-zero term (rational).

## Side comment — alternative parametrizations:

- Garcia-Martin et al. [PRD 83 (2011)]:  $\pi\pi/K\bar{K}$  up to 1.4 GeV with the analyticity constant.
- Ropertz et al. [EPJ C78 (2018)]: K-matrix extension of (above) up to 2.5 GeV (with three channels  $\pi\pi/K\bar{K}/4\pi$ ) fit to LHCb data on  $B_s \rightarrow J/\psi\pi\pi$  decay.

# Extracted $(\pi\pi)_S$ production amplitude

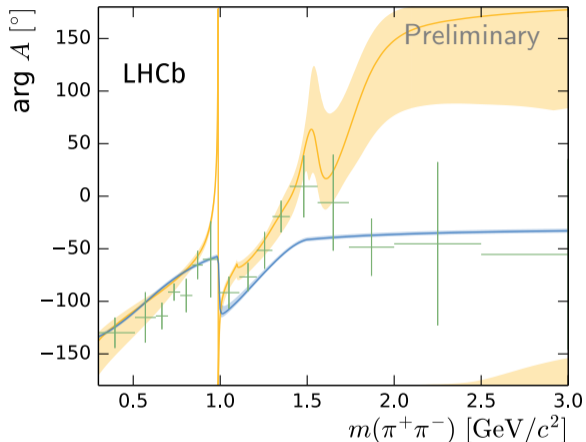
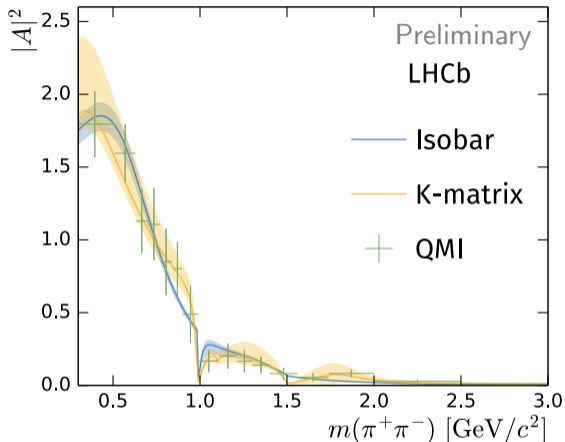
[PAPER-2019-017 (LHCb)]



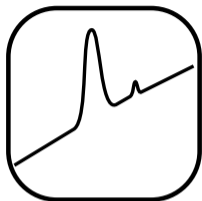
- Clear difference in  $(\pi\pi)_S$  amplitude in  $B^+$  and in  $B^-$

# Extracted $(\pi\pi)_S$ production amplitude

[PAPER-2019-017 (LHCb)]



- Clear difference in  $(\pi\pi)_S$  amplitude in  $B^+$  and in  $B^-$
- Different parametrizations are broadly consistent to each other



# Observation of new $\Lambda_b$ states

[arXiv:1907.13598]

- kinematic fits, BDT, spectrum fit, amplitude analysis

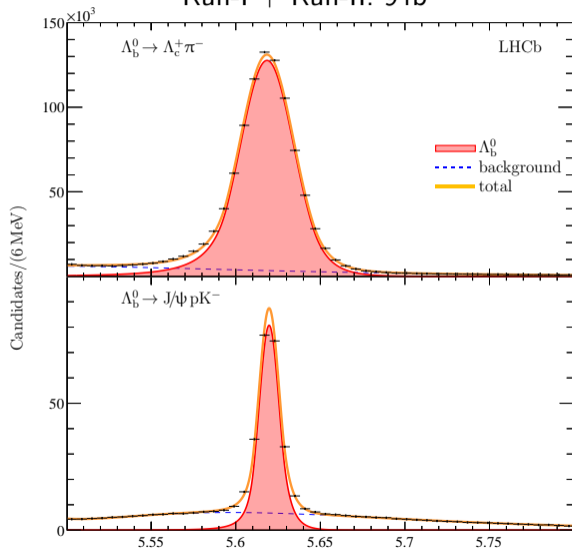
# $\Lambda_b$ combined with $\pi^+\pi^-$

Excitation at the primary vertex

- 900k  $\Lambda_b$  candidates in  $\Lambda_c(\rightarrow pK\pi)\pi$
- Alternative decay channel  $\Lambda_b \rightarrow J/\psi Kp$

[arXiv:1907.13598]

Run-I + Run-II:  $9 \text{ fb}^{-1}$

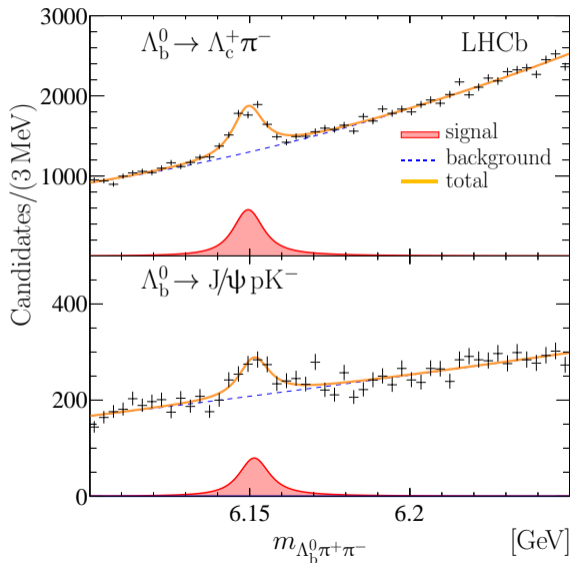


# $\Lambda_b$ combined with $\pi^+\pi^-$

Excitation at the primary vertex vertex

- 900k  $\Lambda_b$  candidates in  $\Lambda_c(\rightarrow pK\pi)\pi$
- Alternative decay channel  $\Lambda_b \rightarrow J/\psi Kp$
- Structure in  $\Lambda_b\pi\pi$  around 6.15 GeV

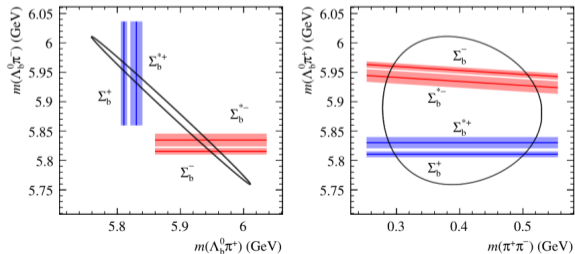
[arXiv:1907.13598]



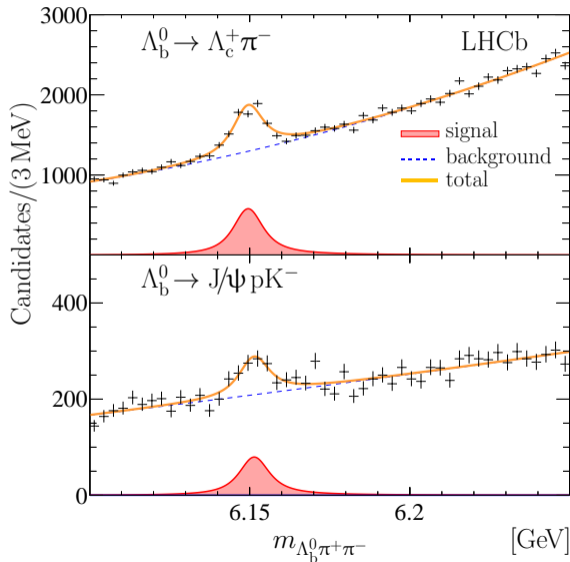
# $\Lambda_b$ combined with $\pi^+\pi^-$

Excitation at the primary vertex

- 900k  $\Lambda_b$  candidates in  $\Lambda_c(\rightarrow pK\pi)\pi$
- Alternative decay channel  $\Lambda_b \rightarrow J/\psi Kp$
- Structure in  $\Lambda_b\pi\pi$  around 6.15 GeV
- $\Sigma_b$  substructures on Dalitz Plot

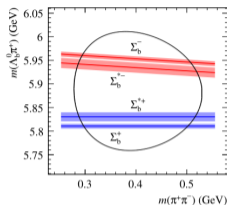


[arXiv:1907.13598]



# Separation by the final state

- Three fit regions:
  - ▶  $\Sigma_b$  region
  - ▶  $\Sigma_b^*$  region
  - ▶ rest (NR region)



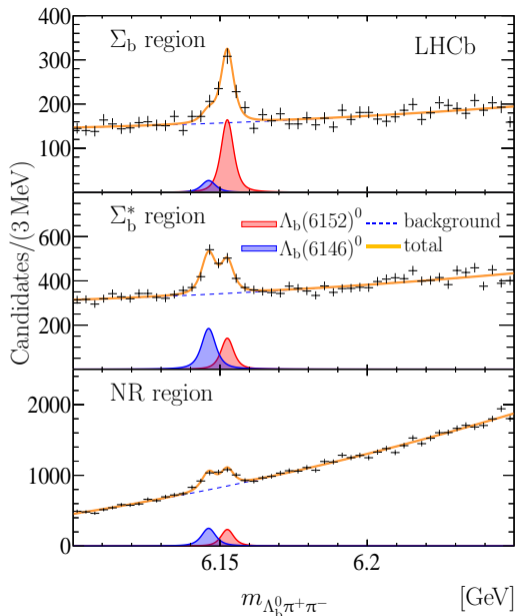
- A simultaneous fit:
  - ▶ Two-signal hypothesis with  $7\sigma$
  - ▶ Almost degenerate narrow states

$$m_{\Lambda_b(6146)^0} = 6146.17 \pm 0.33 \pm 0.22 \pm 0.16 \text{ MeV},$$

$$m_{\Lambda_b(6152)^0} = 6152.51 \pm 0.26 \pm 0.22 \pm 0.16 \text{ MeV},$$

$$\Gamma_{\Lambda_b(6146)^0} = 2.9 \pm 1.3 \pm 0.3 \text{ MeV},$$

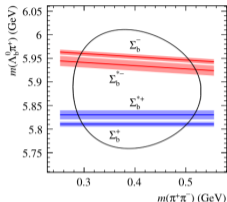
$$\Gamma_{\Lambda_b(6152)^0} = 2.1 \pm 0.8 \pm 0.3 \text{ MeV},$$





# Separation by the final state

- Three fit regions:
  - ▶  $\Sigma_b$  region
  - ▶  $\Sigma_b^*$  region
  - ▶ rest (NR region)



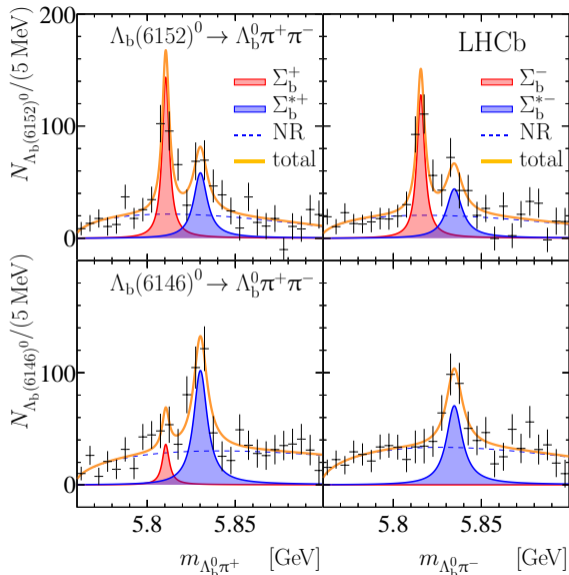
- A simultaneous fit:
  - ▶ Two-signal hypothesis with  $7\sigma$
  - ▶ Almost degenerate narrow states

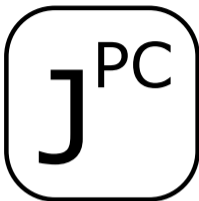
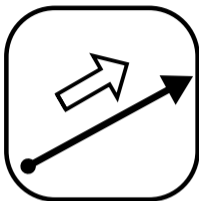
$$m_{\Lambda_b(6146)^0} = 6146.17 \pm 0.33 \pm 0.22 \pm 0.16 \text{ MeV},$$

$$m_{\Lambda_b(6152)^0} = 6152.51 \pm 0.26 \pm 0.22 \pm 0.16 \text{ MeV},$$

$$\Gamma_{\Lambda_b(6146)^0} = 2.9 \pm 1.3 \pm 0.3 \text{ MeV},$$

$$\Gamma_{\Lambda_b(6152)^0} = 2.1 \pm 0.8 \pm 0.3 \text{ MeV},$$





# Quantum numbers and polarization

- investigation of the angular analysis formalism (LHCb+JPAC)  
[EPJ C78 (2018) 727 (JPAC), EPJ C78 (2018) 229 (JPAC), MM et al. (JPAC, in preparation)]

# Conventional helicity approach

Complicated cases: particles with spin in isobar model [Herndon(1975)], [Hansen (1974)]

# Conventional helicity approach

Complicated cases: particles with spin in isobar model [Herndon(1975)], [Hansen (1974)]

$$\underbrace{M_{\{\lambda\}}^\Lambda}_{\text{Diagram 1}} = \underbrace{H_1 D(\phi_1, \theta_1, 0) D(\phi'_1, \theta'_1, 0) W_1(\dots)}_{\text{Diagram 2}} + \underbrace{H_3 D(\phi_3, \theta_3, 0) D(\phi'_3, \theta'_3, 0) W_3(\dots)}_{\text{Diagram 3}} + \underbrace{H_2 D(\phi_2, \theta_2, 0) D(\phi'_2, \theta'_2, 0) W_2(\dots)}_{\text{Diagram 4}}$$

Diagram 1: A central vertex  $M_{\{\lambda\}}^\Lambda$  with an incoming arrow from the left labeled  $p_0, \Lambda$  and index 0. Three outgoing arrows labeled  $p_1, \lambda_1$  (index 1),  $p_2, \lambda_2$  (index 2), and  $p_3, \lambda_3$  (index 3).

Diagram 2: A central vertex  $M_{\{\lambda\}}^\Lambda$  with an incoming arrow from the left labeled  $p_0, \Lambda$  and index 0. Three outgoing arrows labeled  $p_1, \lambda_1$  (index 1),  $p_2, \lambda_2$  (index 2), and  $p_3, \lambda_3$  (index 3). The arrows for  $p_2$  and  $p_3$  are shown as a single line that then splits into two arrows.

Diagram 3: A central vertex  $M_{\{\lambda\}}^\Lambda$  with an incoming arrow from the left labeled  $p_0, \Lambda$  and index 0. Three outgoing arrows labeled  $p_1, \lambda_1$  (index 1),  $p_2, \lambda_2$  (index 2), and  $p_3, \lambda_3$  (index 3). The arrows for  $p_1$  and  $p_2$  are shown as a single line that then splits into two arrows.

Diagram 4: A central vertex  $M_{\{\lambda\}}^\Lambda$  with an incoming arrow from the left labeled  $p_0, \Lambda$  and index 0. Three outgoing arrows labeled  $p_1, \lambda_1$  (index 1),  $p_2, \lambda_2$  (index 2), and  $p_3, \lambda_3$  (index 3). The arrows for  $p_1$  and  $p_2$  are shown as a single line that then splits into two arrows.

- A special set of angles for every decay chain

# Conventional helicity approach

Complicated cases: particles with spin in isobar model [Herndon(1975)], [Hansen (1974)]

$$\underbrace{M_{\{\lambda\}}^\Lambda}_{\text{Diagram 1}} = \underbrace{H_1 D(\phi_1, \theta_1, 0) D(\phi'_1, \theta'_1, 0) W_1(\dots)}_{\text{Diagram 2}} + \underbrace{H_3 D(\phi_3, \theta_3, 0) D(\phi'_3, \theta'_3, 0) W_3(\dots)}_{\text{Diagram 3}} + \underbrace{H_2 D(\phi_2, \theta_2, 0) D(\phi'_2, \theta'_2, 0) W_2(\dots)}_{\text{Diagram 4}}$$

- A special set of angles for every decay chain
- Consistently of quantization

direction – **Wigner rotations**  $W_i(\dots) = D^{j_1}(\tilde{\phi}_1^i, \tilde{\theta}_1^i, 0) D^{j_2}(\tilde{\phi}_2^i, \tilde{\theta}_2^i, 0) D^{j_3}(\tilde{\phi}_3^i, \tilde{\theta}_3^i, 0)$

# The Dalitz-Plot decomposition

[MM (JPAC) in preparation]

Reformulation of the helicity approach

$$p_0, \Lambda \xrightarrow{0} M_{\{\lambda\}}^{\Lambda} \begin{cases} p_1, \lambda_1 \\ p_2, \lambda_2 \\ p_3, \lambda_3 \end{cases} \left. \begin{array}{l} \left. \begin{array}{l} \left. \begin{array}{l} p_1, \lambda_1 \\ p_2, \lambda_2 \end{array} \right\} \sigma_3 \\ \left. \begin{array}{l} p_2, \lambda_2 \\ p_3, \lambda_3 \end{array} \right\} \sigma_1 \end{array} \right\} = \sum_{\nu} \underbrace{D_{\Lambda\nu}^{J*}(\phi_1, \theta_1, \phi_1')}_{\text{Decay-plane orientation}} \times \underbrace{O_{\{\lambda\}}^{\nu}(\sigma_3^2, \sigma_1^2)}_{\text{Dalitz-plot function}}$$

Model-independent factorization of the overall rotation:

- Exploits properties of the Lorentz group (orientation – just three Euler angles)
- Dalitz-plot function depends entirely on 2 variables (no extra azimuthal angles)

# The Dalitz-Plot decomposition

[MM (JPAC) in preparation]

Reformulation of the helicity approach

$$p_0, \Lambda \xrightarrow{0} M_{\{\lambda\}}^{\Lambda} \begin{cases} p_1, \lambda_1 \\ p_2, \lambda_2 \\ p_3, \lambda_3 \end{cases} \left. \begin{array}{l} \sigma_3 \\ \sigma_1 \end{array} \right\} = \sum_{\nu} \underbrace{D_{\Lambda\nu}^{J*}(\phi_1, \theta_1, \phi_1')}_{\text{Decay-plane orientation}} \times \underbrace{O_{\{\lambda\}}^{\nu}(\sigma_3^2, \sigma_1^2)}_{\text{Dalitz-plot function}}$$

Model-independent factorization of the overall rotation:

- Exploits properties of the Lorentz group (orientation – just three Euler angles)
- Dalitz-plot function depends entirely on 2 variables (no extra azimuthal angles)

Gives significant benefits to

- Pentaquark analysis,  $\Lambda_b/\Lambda_c$  polarisation measurements, Baryonic decay chains,...

- proposal for the electromagnetic dipole moments of charged baryons  
[EPJC 77 (2017) 181, arXiv:1708.08483]
- polarization information for complex decay chains

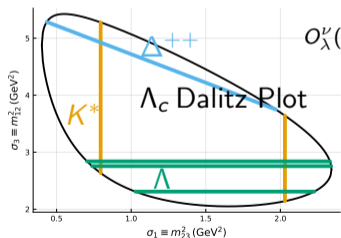


- proposal for the electromagnetic dipole moments of charged baryons  
[EPJC 77 (2017) 181, arXiv:1708.08483]
- polarization information for complex decay chains

$$M_{\lambda}^{\Lambda} = \sum_{\nu} D_{\Lambda\nu}^{1/2*}(\phi_1, \theta_1, \phi_{23}) O_{\lambda}^{\nu}(\sigma_1, \sigma_3),$$

- proposal for the electromagnetic dipole moments of charged baryons [EPJC 77 (2017) 181, arXiv:1708.08483]
- polarization information for complex decay chains

$$M_\lambda^\Lambda = \sum_\nu D_{\Lambda\nu}^{1/2*}(\phi_1, \theta_1, \phi_{23}) O_\lambda^\nu(\sigma_1, \sigma_3),$$



$$O_\lambda^\nu(\sigma_1, \sigma_3) = \sum_s \sum_\tau H_{\tau,\lambda}^{0 \rightarrow (23),1} d_{\nu,\tau-\lambda}^{1/2}(0) X_s(\sigma_1) H_{0,0}^{(23) \rightarrow 2,3} d_{\tau,0}^s(\theta_{23})$$

$$+ \sum_s \sum_{\tau,\lambda'} H_{\tau,0}^{0 \rightarrow (31),2} d_{\nu,\tau}^{1/2}(\hat{\theta}_{2(1)}) X_s(\sigma_2) H_{0,\lambda'}^{(31) \rightarrow 3,1} d_{\tau,-\lambda'}^s(\theta_{31}) d_{\lambda',\lambda}^{1/2}(\tilde{\theta}_{2(1)}^1)$$

$$+ \sum_s \sum_{\tau,\lambda'} H_{\tau,0}^{0 \rightarrow (12),3} d_{\nu,\tau}^{1/2}(\hat{\theta}_{3(1)}) X_s(\sigma_3) H_{\lambda',0}^{(12) \rightarrow 1,2} d_{\tau,\lambda'}^s(\theta_{12}) d_{\lambda',\lambda}^{1/2}(\tilde{\theta}_{3(1)}^1).$$

Couplings ( $H$ ) and lineshapes ( $X$ ) are only model-dependent inputs

## Summary

- LHCb collected  $9 \text{ fb}^{-1}$  (Run-I + Run-II)
- It has already impacted spectroscopy and a lot to be discovered (Run-II)

### Well-established tool chain:

- PID, momentum scaling, kinematic fitters are built in standardized programs,
- Active usage of ML frameworks,
- Good understanding of the spectra lineshapes,
- Wide spectrum of frameworks for angular analysis,
- High standard for systematic checks.

+ active cooperation with theory groups

## Summary

- LHCb collected  $9 \text{ fb}^{-1}$  (Run-I + Run-II)
- It has already impacted spectroscopy and a lot to be discovered (Run-II)

### Well-established tool chain:

- PID, momentum scaling, kinematic fitters are built in standardized programs,
- Active usage of ML frameworks,
- Good understanding of the spectra lineshapes,
- Wide spectrum of frameworks for angular analysis,
- High standard for systematic checks.

+ active cooperation with theory groups

⇒ Great results with intense rate



Thank you for the attention